 doi:10.20944/preprints201709.0095.v1

Effect of Microstructure on the Thermal Conductivity of Plasma Sprayed Y_2O_3 Stabilized Zirconia (8 %YSZ)

Ningning Hu, Matiullah Khan, Yongzhe Wang, Xuemei Song, Yi Zeng
Emails: NingnHu@163.com, matiullahustb@gmail.com, wangyongzhe@mail.sic.ac.cn, songxuemei@mail.sic.ac.cn, zengyi@mail.sic.ac.cn
The State Key Lab of High Performance Ceramics and Superfine Microstructure, Shanghai Institute of Ceramics, Chinese Academy of Sciences, Shanghai 200050, China

Abstract
In this paper, the effect of microstructure on the thermal conductivity of plasma-sprayed Y_2O_3 stabilized ZrO_2 (YSZ) thermal barrier coatings (TBCs) is investigated. Nine freestanding samples deposited on aluminum-base superalloy are studied. Cross-section morphology such as pores, cracks, m-phase content, grain boundary density of the coated samples are examined by scanning electron microscopy (SEM) and electron back-scattered diffraction (EBSD). Multiple linear regressions are used to develop quantitative models which describe the relationship between the particle parameters, m-phase content and the microstructure such as porosity, crack-porosity, the length density of small-angle-crack and the length density of big-angle-crack. Moreover, the relationship between microstructure and thermal conductivity is investigated. Results reveal that the thermal conductivity of the coating is mainly determined by the microstructure and grain boundary density at room temperature (25 ℃) and by the length density of big-angle-crack, monoclinic phase content and grain boundary density at high temperature (1200 ℃).

Keywords: thermal barrier coatings; 8 %YSZ; thermal conductivity; microstructure.

1. Introduction

Yttria-stabilized zirconia (YSZ) is widely used to protect the high temperature components from corrosion and improve the operating temperature of gas-turbine engine. The main aim is to reduce the thermal conductivity of engine components by using YSZ material prepared by atmospheric plasma spray (APS) method [1,2]. The spraying parameters and deposition efficiency in the plasma process produce variety of microscopic defects having pores and cracks which appear in the coatings [3-5]. The microscopic defects have great influence on the thermal conductivity of TBCs [6].

Preprints (www.preprints.org) | NOT PEER-REVIEWED | Posted: 20 September 2017 doi:10.20944/preprints201709.0095.v1

Recently, advanced instrumentations made it possible to observe and measure the movement of particles in the spray state [7,8] from the velocity and temperature of in-flight particles in the drying spray. Many researchers have studied the relationship between the thermal conductivity and the microstructure. Studies shows that cracks parallel to the direction of the matrix and pores can effectively reduce the thermal conductivity while cracks vertical to the direction of the matrix increases the heat transfer[9-11]. The amount of different phase contents of the TBCs will have varying impact on the thermal conductivity. The thermal conductivity of monoclinic zirconia is higher than the tetragonal and cubic phases [11-13]. Some studies investigated the relationship between the spray process and the microstructure of the thermal barrier coating [14,15]. It was found that with increasing particle velocity and temperature the coating is densified and the thermal conductivity increases [14,15]. The quantitative effect of grain boundaries on the thermal conductivity was analyzed which shows that the thermal conductivity of small grains is lower compared to large grains[16-18].

Unfortunately, many microstructural studies failed to corporate the complementary methods to characterize or quantify the bulk behavior. Only the commonly reported microstructures have been associated with the different stages of the phase evolution process, however, to build a more comprehensive understanding of the underlying mechanisms, a detail study is required.

In this manuscript, the effect of microstructure on the thermal conductivity of 8 %YSZ thermal barrier coatings (TBCs) is evaluated. Using scanning electron microscopy (SEM) and electron back-scattered diffraction (EBSD), the cross-section morphology such as pores, cracks, m-phase content and grain boundary density of the coated samples are studied and general relationship about the microstructure and thermal conductivity is developed.

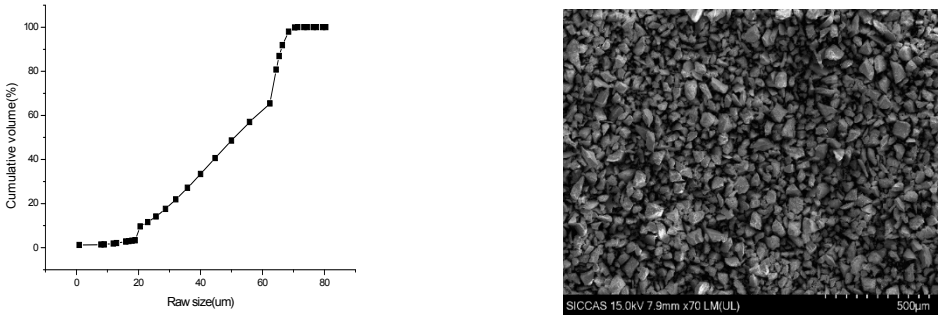

(a) (b)

Fig. 1 (a) Powder morphology and (b) raw size distribution of feeding powders.

Preprints (www.preprints.org) | NOT PEER-REVIEWED | Posted: 20 September 2017 doi:10.20944/preprints201709.0095.v1

2. Experiments

2.1 Materials and preparation

The Metco A-2000 atmospheric plasma spray with a F4-MB plasm gun (Sulzer Metco AG, Switzerland) is used to deposit coatings on aluminum substrates (130 mm x 85 mm x 3 mm). The ceramic powder used for top coats was commercially ZrO_2–8 wt.% Y_2O_3. Fig. 1 demonstrates the power morphology and raw size of the raw material. The medium size（D_{50}） of the powder is 50.9. Thick free-standing coatings（about 1 mm）for thermal properties are deposited using different parameters as summarized in Table 1.

The in-flight parameters of velocity and temperature for depositing sample on the substrate are measured by online monitoring system (Spray Watch 2i, OSEIR, Finland). Under the control of computer, different parameters are measured.

Table 1 Plasma spray parameters and particle velocity and temperature.

	N1	N2	N3	N4	N5	N6	N7	N8	N9
Current (A)	550	550	550	600	600	600	650	650	650
Ar (L/min)	35	40	36	35	40	36	35	40	36
H_2 (L/min)	7	10	12	7	10	12	7	10	12
Velocity（m/s）	197	217	219	206	213	228	214	205	237
Temperature（℃）	2750	2931	3145	2835	3007	3221	2903	3079	3294

2.2 Microstructure characterization

Microstructure of TBCs is characterized qualitatively by microstructure observation and quantitatively by Image Pro Plus (IPP) technique by gray level variation. Pores appear very dark, which permit to be distinguished and quantified by image analysis. In this paper, the direct examination of coatings microstructure from cross-section of the coatings using a scanning electron microscopy (SEM) gives comparative information about porosity of the different coatings. The SEM system（Magellan 400，FEI, USA） equipped with EBSD (INCA SERIES, Oxford Instrument, UK) is used for this purpose. In conjunction with EBSD detector, the phase compositions and grain information of the microstructure are shown in the images.

Based on the SEM-EBSD system for the microstructure and phase compositions, the

Preprints (www.preprints.org) | NOT PEER-REVIEWED | Posted: 20 September 2017 doi:10.20944/preprints201709.0095.v1

phases and grain size were chosen for EBSD analysis. In the area surrounding the top coating interface, a phase with grain information map was constructed using a phase component in the software (Figures 2a and 2b). This map presents the phase distributions and grain information in the polishing- cross-section of the TBCs.

2.3 Thermal conductivity measurements

The TBCs are removed from the substrate for polishing into small diameters of 10 mm and 5 mm that could be used for thermal diffusion and specific heat capacity tests，respectively. The thermal diffusivity (α) is measured using a laser flash method with the temperature range of 25 – 1200 ℃. The specific heat capacity (C_p) of TBCs is tested using the ASTME1269-05 standard from room temperature to 500 ℃. Above 500℃, the specific heat capacity was calculated by using the Neumann-Kopp law(). The density (ρ) of coatings is determined using Archimedes principle. Hence, the thermal conductivity (λ) was calculate by the equation

$$\Lambda = \alpha\rho Cp$$

where α, ρ and Cp are the thermal diffusivity, density and specific heat of the coatings, respectively.

3. Results and discussion

3.1 Spray parameters and phase content

The spray parameters, the temperature and velocity of particles of the nine TBCs are listed in Table 1. The content of m-phase and grain boundary density is shown in Fig. 1. Relationship between m-phase and spraying parameters can be achieved from the content of m-phase showing an incremental trend. The A_2 and H_2 influenced the in-flight particle velocity and current and H_2 influenced the particle temperature. However, high current and H_2 will provide greater energy to the particles and it will melt out. Therefore, the m-phase content of the coating during the cooling process should be higher. Comparing Table 1 and Table 2, it is found that as the particle energy increases then as a result the m-phase will relatively increase. During the spray cooling process, t-phase is found to evolve into a martensitic transformation into m-phase at around 950 ℃, resulting in a volume increase and promoting the increase of Nano - microscopic defects such as cracks and pores. In Fig. 2(a), the coating contain coarse grains (the powder size is 5 μm), columnar grains (aspect ratio > 2), and a large number of small equiaxed grains (20-500 nm). The grain boundary density is inversely related to the grain size, with the decrease in grain size, the grain boundary density increases, as verified from Table 2. Due to the limitations of plasma spraying properties, the effect of spray parameters on grain boundary density is not significant.

Preprints (www.preprints.org) | NOT PEER-REVIEWED | Posted: 20 September 2017 doi:10.20944/preprints201709.0095.v1

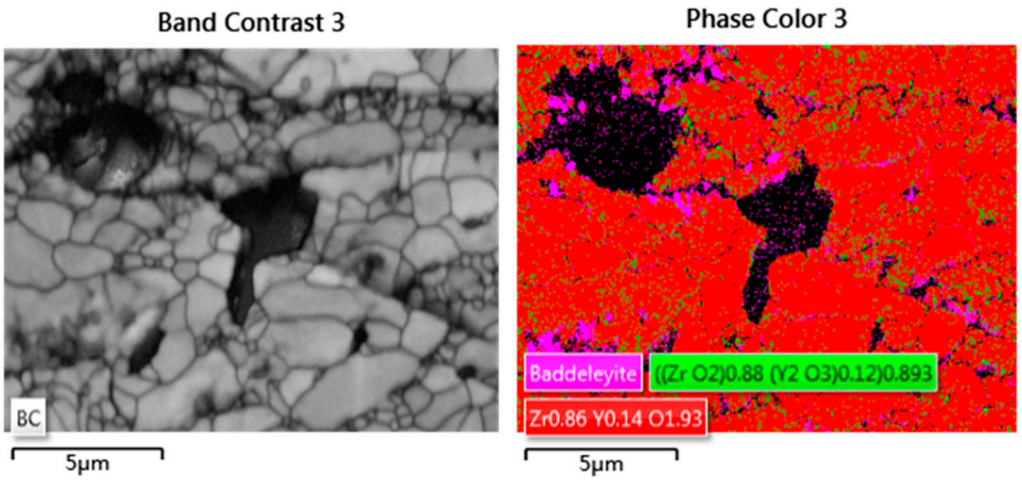

(a) (b)

Fig. 2 EBSD mappings of cross sections (a) grain boundary and (b) the phases distribution

Table 2 Coating parameters

	N1	N2	N3	N4	N5	N6	N7	N8	N9
m-ZrO_2 content （%）	1.026	1.37	1.51	1.55	1.466	1.95	1.9	2.735	2.85
Grain boundary density(m/μm^2)	2.59	2.56	2.61	3.48	2.29	2.87	1.42	3.43	2.43

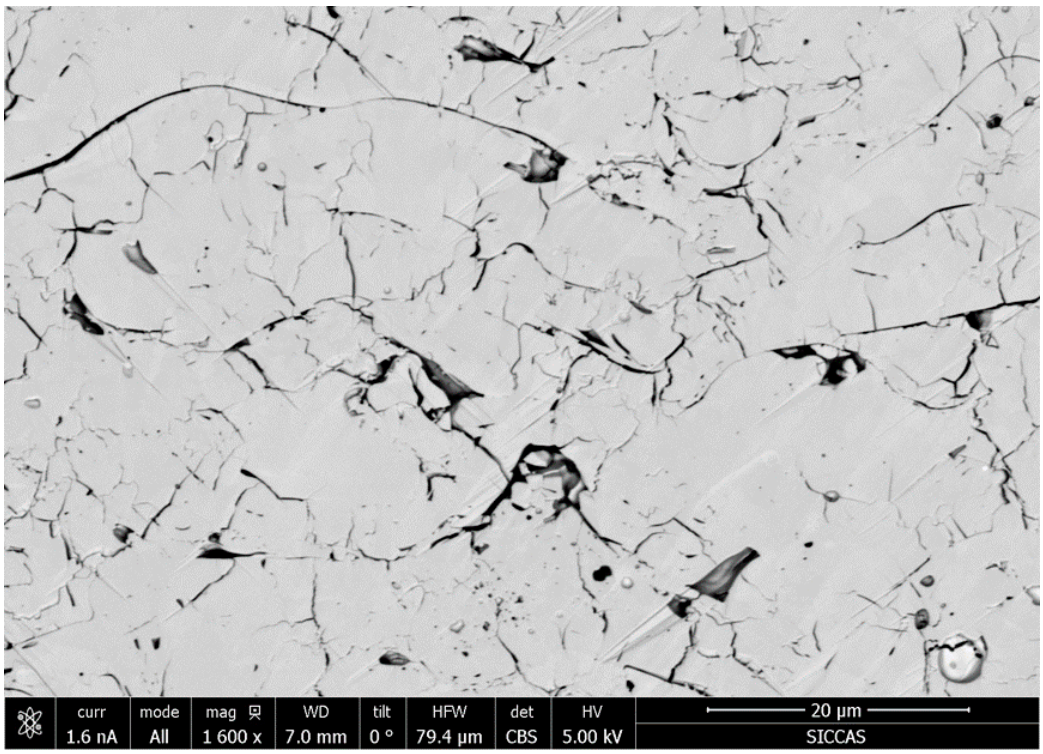

Fig. 3 SEM image of polished cross-sections of APS coating.

Preprints (www.preprints.org) | NOT PEER-REVIEWED | Posted: 20 September 2017 doi:10.20944/preprints201709.0095.v1

3.2 Microstructure of TBCs

Fig. 3 displays the SEM image profile of the thermal barrier coating for atmospheric plasma spraying. A variety of pores and cracks could be clearly distinguished. Therefore, the qualitative and quantitative analysis of microstructure of coatings using SEM micrograph of mirror-polished cross-section is analyzed. In the image analysis, every pore of the maximum diameter "a" and minimum diameter "c" were measured to calculate the ratio a/c. If the ratio is < 3 then it can be described as pores and if it is > 3 then it can be considered as cracks. Furthermore, more meticulous work on cracks is done in which the angle of each crack and the length of each type crack is measured. The angle from 0° - 45° is named as small-angle-cracks while the 45° - 90° are referred as big-angle-cracks. Finally, the length of density of the two kinds of cracks is calculated. Using the atmospheric plasma spray (APS) to heat the YSZ powder and then spray on the substrate, the particles achieve high temperature and speed. High-energy particles in the spraying process in the matrix create variety of defects and it is found that the spraying process greatly influence the evolution of different phases content. In Fig. 2 (b), it is clear that the m-phase appears around large pores and small-angle cracks. This is due to rapid cooling. The tetragonal phase transform into monoclinic phase accompanied by volume change. When the pressure in the pores and cracks is minimal the t-phase easily transforms to m-phase, but the pressure inside the coating is too large to transform, so the monoclinic phase is mainly distributed around the pores and cracks. T-phase evolves to m-phase transition, with about 3 – 5 % of volume expansion, and m-phase transform to t-phase with about 7 % of volume shrinkage. At about 950 ℃, the t-phase will transform to m-phase having volume expansion of 3%-5 %. The linear regression equation shows that the pores and cracks and the length density of small-angle-crack of the coating are strongly correlated with the spray parameters and the monoclinic content.

Preprints (www.preprints.org) | NOT PEER-REVIEWED | Posted: 20 September 2017 doi:10.20944/preprints201709.0095.v1

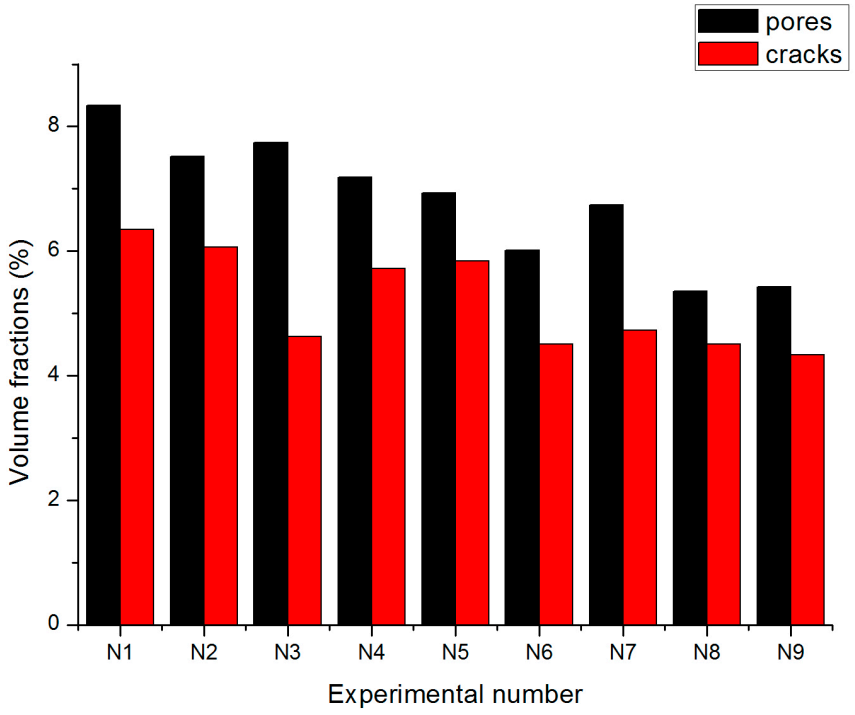

(a)

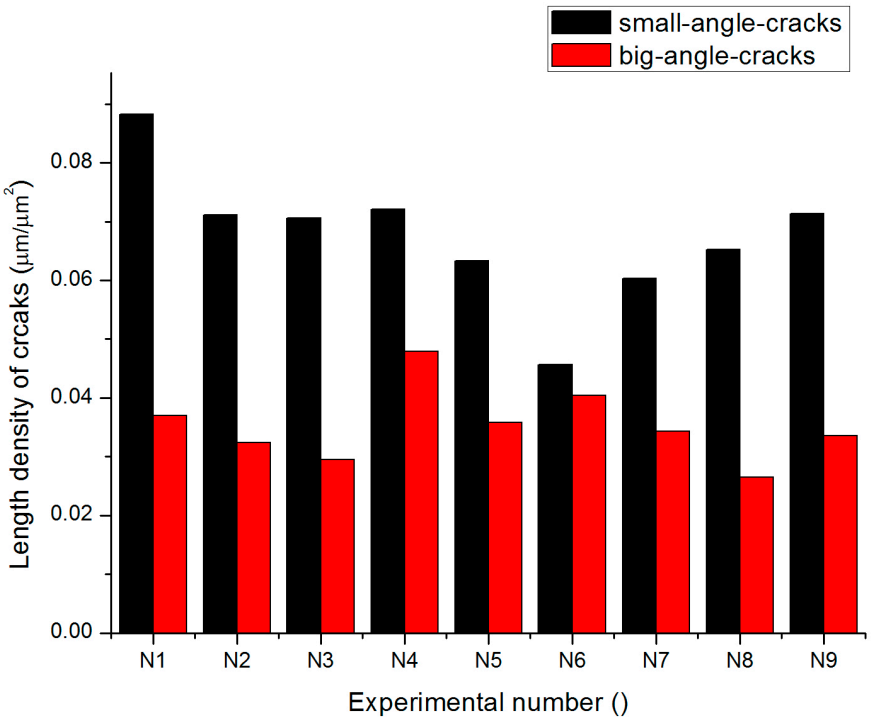

Fig. 3 (a) Volume fractions of pores and cracks (b) length density of cracks

Preprints (www.preprints.org) | NOT PEER-REVIEWED | Posted: 20 September 2017 doi:10.20944/preprints201709.0095.v1

Porosity (%)

$$=10.825-0.00014X_1-0.00042X_2-1.499X_3 \qquad R^2=0.90 \qquad (1)$$

Crack-porosity (%)=

$$14.599-0.015816965X_1-0.001496453X_2-0.878686315X_3 \qquad R^2=0.79 \qquad (2)$$

Length Density of Small-angle-cracks (μ m/ μ m^2)

$$=0.215790122-0.000371226X_1-0.00000980847X_2-0.026043962X_3 \qquad R^2=0.91 \qquad (3)$$

Length Density of Big-angle-cracks (μ m/ μ m^2)

$$=0.049720041+0.000355754X_1-2.94618\times10^{-5}X_2-0.001130176X_3 \qquad R^2=0.27 \qquad (4)$$

where X_1 is particle velocity，X_2 is the temperature of particles，and X_3 is the content of m-phase.

Equ. 1 and 2 gives that particle velocity, temperature, respectively. The m-phase contents are determined from the porosity and crack-porosity of coatings. It can be concluded that increasing the speed and temperature of particles then the m-phase content would be reduced leading to the reduction in porosity and crack-porosity. Equation 3 describes these parameters which determine the length density of small-angle-crack. A very small m-phase near the large-angle-cracks is found and experiments show that the relative formation of cracks and pores in the m-phase play negative role. During cooling process, the volume change of t-phase to m-phase leads to further reduction in the pores and cracks. However, spray parameters have small influence on the big-angle-cracks. Equation 4 shows that as R^2 is too small then the correlation between the length density of big-angle-cracks and the parameters is very small. Since the generation of the length density of big-angle-cracks in the spraying process results from the release of stress, the big-angle-cracks are more random and smaller.

3.3 Relationship between microstructure and thermal conductivity relationship

In Fig. 4, the thermal conductivity of TBCs at room temperature and 1200 ℃ are compared. At 25 degrees, the thermal conductivity is significantly higher than the 1200 degrees. It is due to the fact that the influence factor of thermal conductivity at low and high temperature is mainly caused by the change of average free path of phonons in YSZ heat conduction process at low and high temperature. The

Preprints (www.preprints.org) | NOT PEER-REVIEWED | Posted: 20 September 2017 doi:10.20944/preprints201709.0095.v1

relationship between microstructure and thermal conductivity from the multiple regression equations at low and high temperature are given as follows:

Thermal conductivity (room temperature) =

1.79-0.104864402P-0.038644461C-0.009469272S+23.24351385B-0.170350528G

R^2=0.82 (5)

Thermal conductivity (1200℃) =

0.476267554+21.50434266B+0.092513106M-0.168259582G R^2=0.888 (6)

where P is the porosity, C is the crack-porosity, S is the length density of small-angle-crack, B is the length density of big-angle-crack, and G is the grain boundary density.

In Equ. 5, at low temperatures, pores, cracks, and the length density of small-angle-cracks increase the phonon scattering and effectively reduce the thermal conductivity. However, the length density of big-angle-cracks will lead to the heat flow into the depths of the layer, thereby promoting the phonon heat transfer leading to enhanced thermal conductivity. Moreover, more pores and cracks in the YSZ coatings might not have the decisive factor of reducing the thermal conductivity, suggesting that the other microstructural features also have significant influence on the thermal conductivity. Grain boundaries are also one of the important sources of phonon scattering. The small grain boundary size results in large grain boundary density that increases the intensity of phonon scattering and thus leads to a lower thermal conductivity.

At high temperature (1200℃), the average free path of the phonon decreases, and the mean free path of the phonon is close to several lattice spacing, so the larger the grain boundary density is, the phonon scattering will be more stronger. Furthermore, the pores are too large and it cannot be ignored. M-phase has a significant effect at high temperature, with the increase in M-phase contents, the thermal conductivity of the coatings increases. In Equ. 4 and 5, the length of big-angle-crack both have large coefficient and it mean that it could strongly influence the thermal conductivity. Compared with other factors, the lengths of big-angle-cracks have also large impact on the thermal conductivity, because both at low and high temperature heat flow it can directly access inside the coating.

Preprints (www.preprints.org) | NOT PEER-REVIEWED | Posted: 20 September 2017 doi:10.20944/preprints201709.0095.v1

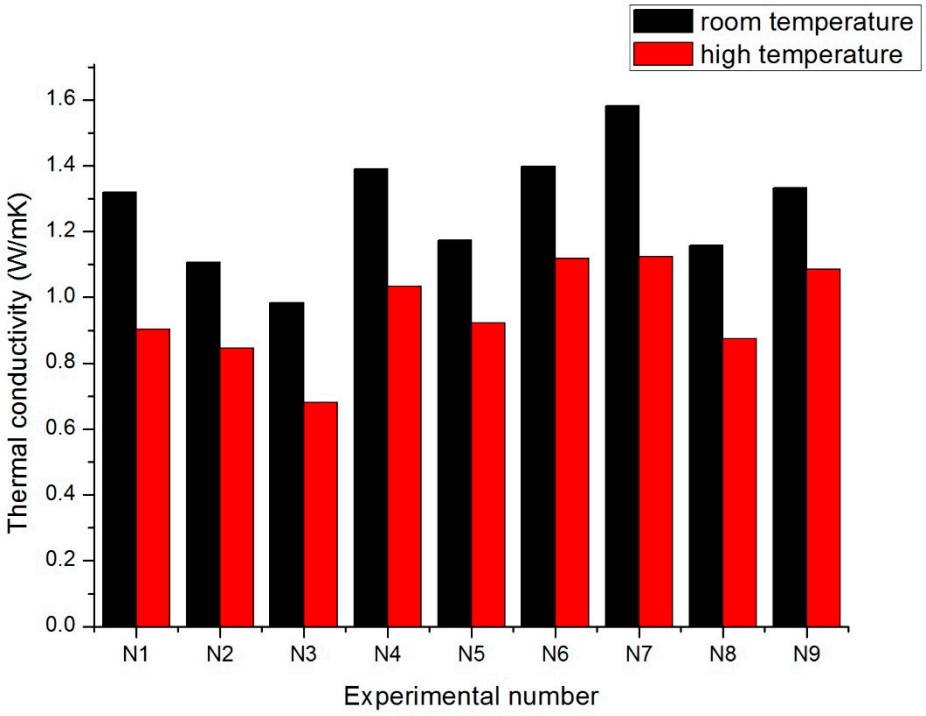

Fig. 4 Thermal conductivity of APS coatings at 25℃ and 1200℃

4. Conclusions

(1) Spraying process affect the m phase content of the coating and increasing the spray parameters of the coating lead to improvement in the m phase content.

(2) The volume change of the phase transition during the spraying process affect the microstructure of the coating. M-phase content and the in-flight particle state play significant role in the formation of micro-morphology. The formation of the length of big-angle-crack resulted from the stress release and generally very small and random distribution.

(3) At low temperature (25 ℃), the influence of thermal conductivity on pores, cracks, the length of small-angle-crack and grain boundary density decrease the thermal diffusion but the big-angle-crack increase the heat flow to the coating. At high temperatures, the effects of pores and cracks are negligible. The grain boundary density reduces the thermal diffusion. The effects of big-angle-cracks on heat diffusion at both low and high temperatures are enormous.

 doi:10.20944/preprints201709.0095.v1

References

1.Akwaboa S, Mensah P, Diwan R. Effects of Thermal Radiation on Air Plasma Spray (APS) Coated Gas Turbine Blade[C]// ASME Turbo Expo 2010: Power for Land, Sea, and Air. 2010:627-633.

2.Chen Z. Hot corrosion and high-temperature deformation of yttria-stabilized zirconia thermal barrier coatings[J]. 2006.

3.Masoule S T, Valefi Z, Ehsani N. Effect of plasma spray parameters on microstructure and thermal conductivity of APS TBC YSZ[C]// Imat. 2014.

4.Lee S Y, Kwon J Y, Kang T W, et al. Effects of Thickness on Thermal and Mechanical Properties of Air-Plasma Sprayed Thermal Barrier Coatings[C]// Materials Science Forum. 2010:372-375.

5.Liu H, Jazi H R S, Bussmann M, et al. Experiments and modeling of rapid solidification of plasma-sprayed yttria-stabilized zirconia[J]. Acta Materialia, 2009, 57(20):6013-6021

6.Chi W, Sanjay Sampath, Wang H. Microstructure–Thermal Conductivity Relationships for Plasma-Sprayed Yttria-Stabilized Zirconia Coatings[J]. Journal of the American Ceramic Society, 2008, 91(8):2636–2645.

7.Zhao L, Bai Y, Tang J J, et al. Effect of particle in-flight behavior on the composition of thermal barrier coatings[J]. Applied Surface Science, 2013, 286(12):184-191.

8.Cheng D, Xu Q, Lavernia E J, et al. The effect of particle size and morphology on the in-flight behavior of particles during high-velocity oxyfuel thermal spraying[J]. Metallurgical & Materials Transactions B, 2001, 32(3):525-535.

9.R. Vaßen, N. Czech, W. Malléner, et al. Influence of impurity content and porosity of plasma-sprayed yttria-stabilized zirconia layers on the sintering behaviour[J]. Surface & Coatings Technology, 2001, 141(2):135-140.

10.Arai M, Ochiai H, Suidzu T. A novel low-thermal-conductivity plasma-sprayed thermal barrier coating controlled by large-pores[J]. Surface & Coatings Technology, 2016, 285:120-127.

11.Song X, Liu Z, Suhonen T, et al. Effect of melting state on the thermal shock resistance and thermal conductivity of APS ZrO 2 –7.5 wt.% Y 2 O 3, coatings[J]. Surface & Coatings Technology, 2015, 270(120):132-138.

12.S. Wei, W. Fu-chi, F. Qun-Bo, and M. Zhuang, Effects of Defects on the Effective Thermal Conductivity of Thermal Barrier Coatings, Appl. Math. Model., 2012, 36(5), p 1995-2002

13. Raghavan S, Wang H, Dinwiddie R B, et al. The effect of grain size, porosity and yttria content on the thermal conductivity of nanocrystalline zirconia[J]. Scripta Materialia, 1998, 39(8):1119-1125.

 doi:10.20944/preprints201709.0095.v1

14.G. Dwivedi et al., Assessing Process and Coating Reliability Through Monitoring of Process and Design Relevant Coating Properties, J. Therm. Spray Technol., 2010, 19(4), p 695-712

15. C. Zhang et al., Effect of in-Flight Particle Velocity on the Performance of Plasma-Sprayed YSZ Electrolyte Coating for Solid Oxide Fuel Cells, Surf. Coat. Technol., 2008, 202(12), p 2654-
2660

16.Soyez G, Eastman J A, Thompson L J, et al. Grain-size-dependent thermal conductivity of nanocrystalline yttria-stabilized zirconia films grown by metal-organic chemical vapor deposition[J]. Applied Physics Letters, 2000, 77(8):1155-1157.

17.Limarga A M, Clarke D R. The grain size and temperature dependence of the thermal conductivity of polycrystalline, tetragonal yttria-stabilized zirconia[J]. Applied Physics Letters, 2011, 98(21):211906-211906-3.

18.Yang H S, Eastman J A, Thompson L J, et al. Grain-size-dependent thermal transport properties in nanophase yttria-stabilized zirconia.[J]. Office of Scientific & Technical Information Technical Reports, 2001.